Development 135, 1703-1711 (2008) doi:10.1242/dev.015248

Dynamic regulation of the expression of neurotrophin receptors by Runx3

Souichiro Nakamura[1,*], Kouji Senzaki[1,*], Masaaki Yoshikawa[1], Mika Nishimura[1], Ken-ichi Inoue[2], Yoshiaki Ito[2], Shigeru Ozaki[1] and Takashi Shiga[1,†]

Sensory neurons in the dorsal root ganglion (DRG) specifically project axons to central and peripheral targets according to their sensory modality. However, the molecular mechanisms that govern sensory neuron differentiation and the axonal projections remain unclear. The Runt-related transcription factors, Runx1 and Runx3, are expressed in DRG neuronal subpopulations, suggesting that they might regulate the cell specification and the trajectories of specific axons. Here, we show that parvalbumin-positive DRG neurons fail to differentiate from the onset in *Runx3*$^{-/-}$ mice. By contrast, TrkC-positive DRG neurons differentiate normally at embryonic day (E) 11.5, but disappear by E13.5 in *Runx3*$^{-/-}$ mice. Subsequently, TrkC-positive DRG neurons reappear but in smaller numbers than in the wild type. In *Runx3*$^{-/-}$ mice, central axons of the TrkC-positive DRG neurons project to the dorsal spinal cord but not to the ventral and intermediate spinal cord, whereas the peripheral axons project to skin but not to muscle. These results suggest that Runx3 controls the acquisition of distinct proprioceptive DRG neuron identities, and that TrkC-positive DRG neurons consist of two subpopulations: Runx3-dependent early-appearing proprioceptive neurons that project to the ventral and intermediate spinal cord and muscle; and Runx3-independent late-appearing cutaneous neurons that project to the dorsal spinal cord and skin. Moreover, we show that the number of TrkA-positive DRG neurons is reduced in *Runx3*$^{-/-}$ mice, as compared with the wild type. These results suggest that Runx3 positively regulates the expression of TrkC and TrkA in DRG neurons.

KEY WORDS: Runx, Transcription factor, Dorsal root ganglion, Proprioceptive neuron, TrkC (Ntrk3), TrkA (Ntrk1), Parvalbumin, Cell fate specification, Axonal projection

INTRODUCTION

Somatosensory information is conveyed from the periphery to the spinal cord by primary sensory neurons located in the dorsal root ganglion (DRG). In the DRG, two major subpopulations of sensory neurons are defined: TrkA (Ntrk1)-expressing (TrkA$^+$) cutaneous neurons, which convey information from thermoreceptors and nociceptors in the skin; and TrkC (Ntrk3)-expressing (TrkC$^+$) proprioceptive neurons, which convey information regarding muscle length and tension (for a review, see Snider, 1994). These distinct sensory neuron subpopulations have different molecular characteristics, and terminate in different laminar targets within the spinal cord and peripheral targets. Trk receptors play crucial roles in neuronal survival, differentiation and axon projection of DRG neurons (Bibel and Barde, 2000; Huang and Reichardt, 2001; Markus et al., 2002; Patel et al., 2003; Snider, 1994). A recent study suggested that the selective expression and signaling of Trk receptors in DRG neurons are involved in axonal target selection in the spinal cord (Moqrich et al., 2004). However, the molecular mechanisms that govern sensory neuron differentiation and the axonal projections remain unclear.

In mammals, the Runt-related (Runx) transcription factor family consists of three members: Runx1, 2 and 3. These Runx transcription factors interact with a common co-factor, polyomavirus enhancer-binding protein 2 [Pebp2; also known as core binding factor β (Cbfβ)] with highly conserved Runt DNA-binding domain that belongs to the Runx transcription factors, and play important roles in developmental processes of various cell types including hematopoietic cells, osteoblasts and gastric epithelial cells (for reviews, see Coffman, 2003; Ito, 2004). Runx1 and Runx3 are also expressed in subtypes of neurons in the peripheral and central nervous systems (Simeone et al., 1995; Theriault et al., 2004; Theriault et al., 2005). In the DRG, reciprocal expression during early stages of development has been reported: Runx1 is initially expressed in TrkA$^+$ presumptive cutaneous neurons, while Runx3 is expressed in TrkC$^+$ presumptive proprioceptive neurons (Chen et al., 2006a; Chen et al., 2006b; Kramer et al., 2006; Levanon et al., 2001; Marmigère et al., 2006). These Runx transcription factors play crucial roles in the cell fate specification and axonal projections of DRG neurons (Chen et al., 2006a; Chen et al., 2006b; Inoue et al., 2002; Kramer et al., 2006; Levanon et al., 2001; Levanon et al., 2002; Marmigère et al., 2006; Yoshikawa et al., 2007) (for a review, see Marmigère and Ernfors, 2007). However, there seem to be some discrepancies concerning the role of Runx3. Inoue et al. showed that TrkC$^+$ DRG neurons are differentiated and maintained, but the projection of proprioceptive axons to both central and peripheral targets is severely impaired in *Runx3*$^{-/-}$ embryos and newborns (Inoue et al., 2002). By contrast, initial appearance and subsequent loss of proprioceptive phenotypes including TrkC expression was reported in DRG neurons of *Runx3*$^{-/-}$ embryos, suggesting the possibility of cell death of proprioceptive DRG neurons (Levanon et al., 2002). More recently, it has been shown that TrkC$^+$ DRG neuron numbers are decreased, with a concomitant increase in TrkB (Ntrk2)-expressing (TrkB$^+$) DRG neurons, in *Runx3*$^{-/-}$ embryos by embryonic day (E) 12.5 (Kramer et al., 2006; Inoue et al., 2007). Runx3 promotes DRG neuron differentiation to a solitary TrkC$^+$ phenotype by repressing TrkB expression in hybrid TrkB$^+$/TrkC$^+$ DRG neurons, and by maintaining the expression of TrkC within prospective proprioceptive DRG neurons (Kramer et al., 2006; Inoue et al.,

[1]Graduate School of Comprehensive Human Sciences, University of Tsukuba, 1-1-1 Tennodai, Tsukuba, Ibaraki 305-8577, Japan. [2]Institute of Molecular and Cell Biology, 61 Biopolis Drive, Proteos, Singapore 138673, Singapore.

*These authors contributed equally to this work
†Author for correspondence (e-mail: tshiga@md.tsukuba.ac.jp)

Accepted 3 March 2008

2007). These findings raise the question as to the role of Runx3 in the control of cell fate specification of proprioceptive DRG neurons, including its role in the expression of TrkC.

In this study, to gain further insight into the function of Runx3 in cell type specification and axonal projections of DRG neurons, we performed a cell fate analysis of *Runx3*$^{-/-}$ dorsal root ganglia (DRGs) during embryonic and neonatal stages. We show that Runx3 is required for the cell fate specification and the axonal projection of proprioceptive DRG neurons. However, a subset of TrkC^{+} DRG neurons appears independently of Runx3 that may subserve cutaneous sensation. Therefore, TrkC^{+} DRG neurons are divided into two subpopulations on the basis of Runx3 dependency: Runx3-dependent early-appearing proprioceptive neurons; and Runx3-independent late-appearing cutaneous neurons. Moreover, we show that Runx3 positively regulates the expression of TrkA and calcitonin gene-related peptide (CGRP; Calca) in addition to TrkC and parvalbumin (PV; Pvalb), suggesting that Runx3 might be involved in the development of cutaneous, as well as of proprioceptive, DRG neurons. Considering our previous study reporting that Runx1 negatively regulates the expression of TrkA, CGRP and TrkC (Yoshikawa et al., 2007), it can be suggested that Runx1 and Runx3 have antagonistic roles in the development of DRG neuron subpopulations.

MATERIALS AND METHODS

Genotyping and maintenance of animals

The strategy used to inactivate *Runx3* in the mouse germline was described previously (Inoue et al., 2002; Li et al., 2002). *Bax*-deficient mice (Knudson et al., 1995) were purchased from the Jackson Laboratory (Bar Harbor, ME). Mice were bred in a clean room in the Laboratory Animal Resource Center at the University of Tsukuba. *Runx3*$^{+/-}$ and *Runx3*$^{+/+}$ mice were obtained from mating of *Runx3*$^{+/-}$ mice. *Runx3*$^{+/-}$; *Bax*$^{+/-}$ double-knockout mice and *Runx3*$^{+/+}$; *Bax*$^{+/-}$ control mice were obtained from the mating of *Runx3*$^{+/-}$; *Bax*$^{+/-}$ double heterozygotes. Timed embryos were obtained by overnight mating, and the morning when the vaginal plug was observed was considered E0.5. For genotyping of *Runx3* deficiency, PCRs were performed using primer pairs for wild-type (NA, 5′-GACTGTGCATGCACCTTT-CACCAA-3′ and CB, 5′-TAGGGCTCAGTAGCACTTACGTCG-3′) or mutant (NA and C2, 5′-ATGAAACGCCGAGTTAACGCCATCA-3′) allele detection. For genotyping of *Bax* deficiency, PCRs were performed using a set of three primers: *Bax* exon 5 forward primer (5′-TGATCAGAAC-CATCATG-3′), *Bax* intron 5 reverse primer (5′-GTTGACCAGAGTG-GCGTAGG-3′) and Neo reverse primer (5′-CCGCTTCCATTGCTCAG-CGG-3′). All experiments followed the Guide for the Care and Use of Laboratory Animals described by the National Institutes of Health (USA), and were approved by the Animal Experimentation Committee of the University of Tsukuba.

Immunohistochemistry

For cryostat sections, E11.5 and E13.5 whole mouse embryos were immersed overnight at 4°C in a fixative containing 4% paraformaldehyde (PFA) in 0.1 M phosphate buffer (PB) (pH 7.4). Embryos at E14.5 and older were perfused transcardially with the same fixative and immersed overnight at 4°C. The trunk at thoracic segments (Th) and lower limbs including the gastrocnemius muscle were dissected and immersed in 30% sucrose in 0.1 M PB and frozen in Tissue-Tek OCT compound (Sakura Finetek, Japan). Ten or 12 μm transverse sections of Th or axial sections of legs were cut and collected onto MAS-coated glass slides (Matsunami Glass, Japan) and air-dried for 1 hour. If needed, sections were subjected to heat-induced epitope retrieval by heating to 105°C for 5 minutes in REAL Target Retrieval Solution (Dako). After treatment for 30 minutes at room temperature (RT) with 0.3% H_2O_2 in methanol, the sections were incubated for 1 hour at RT in a blocking solution containing 1% BSA and 0.1-0.5% Triton X-100 in PBS.

For immunohistochemical analysis, the following antibodies were used: rabbit anti-Runx1 (Sigma; 1:1000 dilution), mouse anti-Runx3 (Abnova; 1:2000), rabbit anti-PV (Swant; 1:2000), goat anti-TrkC (R&D Systems; 1:2500), rabbit anti-calretinin (CR) (Swant; 1:2000), rabbit anti-vesicular glutamate transporter 1 (Vglut1) (a gift from Dr M. Watanabe, Hokkaido University, Sapporo, Japan; 1:1000), mouse anti-Islet1 (Developmental Studies Hybridoma Bank; 1:200), rabbit anti-CGRP (Chemicon; 1:4000), rabbit anti-TrkA (a gift from Dr F. Reichardt, University of California, San Francisco, CA; 1:4000), rabbit anti-TrkB (Upstate; 1:2000), rabbit anti-somatostatin (SOM) (Protos Biotech; 1:2000), rabbit anti-c-Ret (IBL; 1:100) and rabbit anti-calbindin-28K (CB) (Swant; 1:1000). The specificity of antibodies against Runx1 and Runx3 was verified by the absence of immunoreactivity in DRGs of *Runx1*$^{-/-}$ and *Runx3*$^{-/-}$ mice, respectively (Yoshikawa et al., 2007) (data not shown). The sections were incubated for 24-48 hours at 4°C with each of the primary antibodies in the blocking solution. For single staining, the sections were incubated with a biotinylated secondary antibody for 1 hour at RT, followed with the peroxidase-conjugated avidin-biotin complex (Vector Laboratories; 1:100) for 30 minutes at RT. The positive reactions were visualized with 3,3′-diaminobenzidine (DAB) using the ImmunoPure Metal Enhanced DAB Substrate Kit (Pierce). For caspase 3 immunostaining, cryostat sections were incubated with anti-active caspase 3 antibodies (Promega; 1:1000), followed by incubation with Alexa Fluor 488-labeled donkey anti-rabbit IgG (Invitrogen; 1:1000). For double or triple staining, cryostat sections were incubated with anti-Runx3 antibodies, followed by incubation with biotinylated horse anti-mouse IgG (Vector Laboratories; 1:500) and Pacific Blue-conjugated streptavidin (Invitrogen; 1:500). The sections were then incubated with antibody against PV, CR, TrkC, TrkA, TrkB, CGRP or Runx1, followed by Alexa Fluor 488-labeled donkey anti-rabbit or anti-goat IgG, or Alexa Fluor 594-labeled donkey anti-rabbit or anti-goat IgG (Invitrogen; 1:1000). Samples from *Runx3*$^{-/-}$ and *Runx3*$^{+/+}$ littermates were processed simultaneously for immunohistochemistry.

DiI labeling

Newborn mice were deeply anesthetized with diethylether and perfused transcardially with 4% PFA in 0.1 M PB. In order to retrogradely label DRG axons, crystals of a lipophilic fluorescent dye (DiI) were placed in several segments of the thoracic nerves after cutting off the ventral roots. The dyes were allowed to transport for 3 days at 37°C and the preparations were then cut in 50 μm sections for microscopy. Images of DiI-labeled spinal cord were collected on an Axioimager microscope (Carl Zeiss).

Cell counting

For counts of Islet1^{+} DRG neurons, DRGs in the tenth thoracic segment (Th10) at E13.5, E16.5 and postnatal day (P) 0, and for counts of caspase 3^{+} DRG neurons, Th4 DRGs at E17.5 and P0, were serially sectioned at 10 μm. For counts of TrkC^{+}, CR^{+} and PV^{+} DRG neurons, Th10, Th11 and Th12 DRGs from E13.5 to P0, and for counts of Vglut1^{+}, TrkA^{+}, TrkB^{+}, c-Ret^{+}, CB^{+}, SOM^{+} and CGRP^{+} DRG neurons, Th8, Th12, Th6, Th7, Th11, Th12 and Th9 DRGs at P0, were serially sectioned at 10 μm. The number of immunoreactive neurons was determined by counting neurons that contained a nucleus and showed a signal intensity in the cytoplasm >2.5-fold above the noise level in the same sections. The total number of immunoreactive neurons was counted from the level-matched DRGs of each genotype (5-6 DRGs from three animals at each stage were examined).

Measurement of DRG volume

Using serial sections (10 μm) containing whole DRGs (Th10) at E13.5, E16.5 and P0, the areas of the DRG in each section were measured and the DRG volume calculated using AxioVision imaging software (Carl Zeiss).

Measurement of signal intensity of the immunoreactivity of axonal projections in the spinal cord

For measurements of TrkC, PV and Vglut1 immunoreactivity within the spinal cord, Th10, Th11 and Th8 spinal cord, respectively, at P0 were sectioned by cryostat at 10 μm. After immunostaining, images of TrkC, PV and Vglut1 immunoreactive axons in the spinal cord were collected on a LSM510META confocal microscope (Carl Zeiss) or an Axioplan2 imaging microscope (Carl Zeiss). The spinal cord was divided into ten equal parts along the dorsoventral axis and the signal intensity of each part measured using ImageJ (version 1.34s, NIH). The signal intensity of each part in *Runx3*$^{-/-}$ and wild-type spinal cord was quantified by comparison to the total

signal intensity of the whole spinal cord of the wild type. Spinal cord sections from wild-type and *Runx3*$^{-/-}$ littermates were processed simultaneously during the immunohistochemical process, and six spinal cord sections from two to three mice of each genotype were analyzed quantitatively.

Statistical analysis

Quantitative analyses were performed on three pairs of embryos or newborns from three independent pregnant mice. Statistical analyses were performed by ANOVA followed by post-hoc analysis (Fisher's protected least significant difference test). Differences were considered significant if the probability of error was less than 5%. All results were expressed as the mean ±s.e.m.

RESULTS

Decreased number of DRG neurons in *Runx3*$^{-/-}$ mice

First, we examined whether the loss of the *Runx3* gene affects the number of DRG neurons, using Islet1 as a pan-neuronal marker (Fig. 1A-C). The number of Islet1^{+} DRG neurons did not differ in wild-type and *Runx3*$^{-/-}$ mice at E13.5 and E16.5. By contrast, Islet1^{+} DRG neurons were decreased to about 80% of wild-type levels in *Runx3*$^{-/-}$ mice at P0 (Fig. 1C, Table 1). Similarly, the DRG volume did not differ at E13.5 and E16.5, but decreased to about 85% in *Runx3*$^{-/-}$ mice at P0 (Fig. 1D, Table 1). Next, we examined the effects of *Runx3* deficiency on the apoptosis of DRG neurons (Fig. 1E-G). The number of active caspase 3-immunoreactive apoptotic DRG cells did not differ in wild-type and *Runx3*$^{-/-}$ mice at E17.5 (*Runx3*$^{+/+}$, 42.83±3.40 versus *Runx3*$^{-/-}$, 41.33±4.15; n=6) and P0 (4.50±1.98 versus 3.50±1.15; n=6), suggesting that *Runx3* inactivation does not induce caspase 3-dependent apoptosis.

Cell fate specification of proprioceptive DRG neurons in *Runx3*$^{-/-}$ mice

To clarify whether the decrease in the number of *Runx3*$^{-/-}$ DRG neurons was due to the loss of specific neurons, we examined the number of proprioceptive DRG neurons using antibodies against selective markers PV, TrkC and calretinin [CR; calbindin 2 (Calb2)] (Copray et al., 1994; Honda, 1995; Kucera et al., 2002; Mu et al., 1993). In the wild-type mice, PV was expressed at a low level in the DRG (Th12) at E13.5 (data not shown), and subsequently PV expression increased. The number of PV^{+} DRG neurons increased by about 3-fold from E14.5 to E15.5, and thereafter decreased slightly until P0 (Fig. 2A-C,G). By contrast, PV^{+} DRG neurons were virtually absent from E13.5 to P0 in the *Runx3*$^{-/-}$ mice (Fig. 2D-F,G).

Table 1. Number of DRG neurons and volume of DRGs in *Runx3*$^{+/+}$ and *Runx3*$^{-/-}$mice

Stage	*Runx3*$^{+/+}$	*Runx3*$^{-/-}$
Number of Islet1^{+} DRG neurons (Th10)		
E13.5	6791.3±351.0 (6)	6136.8±412.9 (5)
E16.5	6677.3±224.7 (6)	6308.3±502.6 (4)
P0	6647.4±292.5 (5)	5341.5±118.2 (5)*
Volume of DRGs (×10^{5} μm^{3}) (Th10)		
E13.5	78.0±19.0 (5)	91.2±18.9 (5)
E16.5	149.7±3.7 (6)	157.7±3.2 (6)
P0	253.3±7.4 (6)	214.9±5.2 (6)*

Statistical analyses were performed by ANOVA followed by post-hoc analysis (Fisher's protected least significant difference test). Data are presented as mean ±s.e.m. The number of DRGs is shown in parentheses.
*P<0.01.

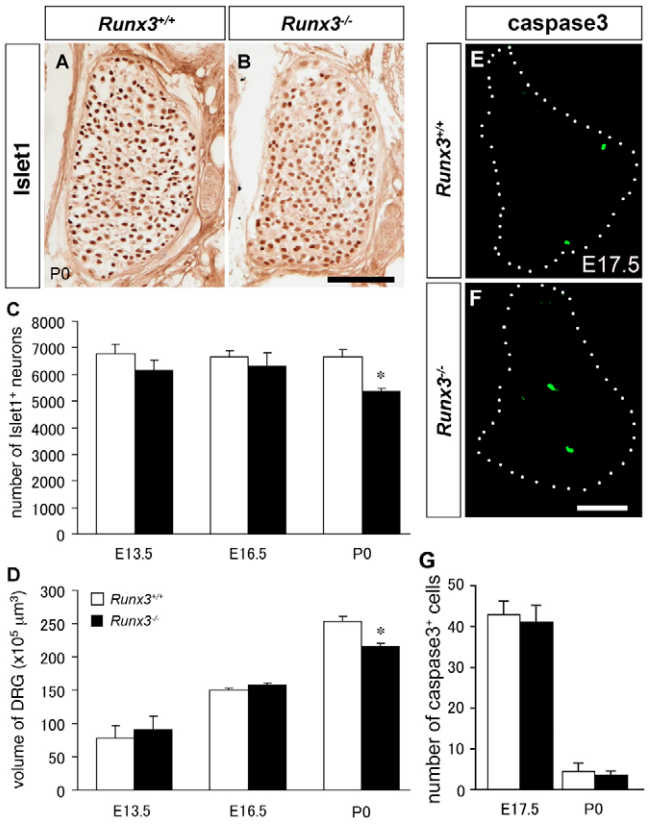

Fig. 1. Number of DRG neurons and DRG volume are decreased in P0 *Runx3*$^{-/-}$ mice with no differences in the number of caspase 3^{+} DRG cells between wild-type and *Runx3*$^{-/-}$ mice. (**A**,**B**) Islet1^{+} neurons in DRGs of wild-type (A) and *Runx3*$^{-/-}$ (B) mice at P0. (**C**,**D**) Quantitative analysis of the total number of Islet1^{+} DRG neurons (C) and the DRG volume (D) at the level of Th10 in wild-type (white bars) and *Runx3*$^{-/-}$ (black bars) mice at E13.5, E16.5 and P0. (**E**,**F**) Immunoreactivity (green) of caspase 3 in DRGs of wild-type (E) and *Runx3*$^{-/-}$ (F) mice at E17.5. The dotted line outlines the DRG. (**G**) Quantitative analysis of the number of caspase 3^{+} DRG cells in wild-type (white bars) and *Runx3*$^{-/-}$ (black bars) mice at E17.5 and P0. Data are shown as mean ±s.e.m.; *P<0.01. Scale bars: 100 μm.

TrkC was expressed in DRGs (Th10) of both the wild-type and *Runx3*$^{-/-}$ mice at E11.5 (Fig. 3A,F). In the wild-type mice, TrkC expression was maintained at E13.5 and the number of TrkC^{+} neurons increased by about 3-fold from E13.5 to E15.5 (Fig. 3B,C,K). By contrast, TrkC^{+} neurons were hardly detected in *Runx3*$^{-/-}$ mice at E13.5 (Fig. 3G,K). TrkC expression reappeared by E14.5 in *Runx3*$^{-/-}$ mice, but the number of TrkC^{+} neurons was significantly smaller than in the wild type (Fig. 3C-E,H-K). At P0, TrkC^{+} neurons were decreased to about 65% in *Runx3*$^{-/-}$ mice (213.2±8.1, n=6, P<0.01) as compared with the wild-type mice (330.0±12.7, n=6) (Fig. 3K). Next, to evaluate the contribution of apoptosis to the disappearance of TrkC^{+} DRG neurons in *Runx3*$^{-/-}$ mice at E13.5, we examined the expression of TrkC in DRGs of *Runx3*$^{-/-}$; *Bax*$^{-/-}$ double-knockout and *Runx3*$^{+/+}$; *Bax*$^{-/-}$ control mice. TrkC expression was maintained in *Runx3*$^{+/+}$; *Bax*$^{-/-}$ but not in *Runx3*$^{-/-}$; *Bax*$^{-/-}$ DRGs at E13.5 (Fig. 1L-O), suggesting that the disappearance of TrkC^{+} DRG neurons is not due to apoptosis.

CR was expressed in a limited number of DRG neurons (see Fig. S1 in the supplementary material). In the wild-type mice, CR was expressed at a low level in DRGs (Th11) at E13.5 and the expression

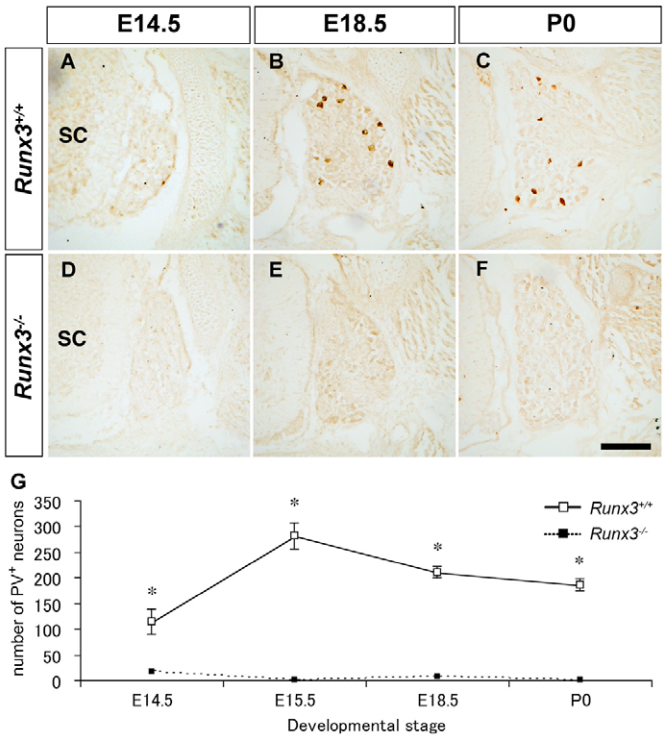

Fig. 2. Loss of expression of parvalbumin in *Runx3*$^{-/-}$ DRGs during development. (**A-F**) Photomicrographs indicate parvalbumin (PV) immunoreactivity (brown) at E14.5 (A,D), E18.5 (B,E) and P0 (C,F) in wild-type (A-C) and *Runx3*$^{-/-}$ (D-F) DRGs at the level of Th12. (**G**) Quantification of PV$^+$ DRG neurons from E14.5 to P0. The number of PV$^+$ neurons in wild-type (white squares) and *Runx3*$^{-/-}$ (black squares) mice are shown, and virtually no neurons express PV in *Runx3*$^{-/-}$ DRGs through these developmental stages. SC, spinal cord. Data are shown as mean±s.e.m.; *P<0.001. Scale bar: 100 μm.

increased subsequently (see Fig. S1A-C in the supplementary material). In *Runx3*$^{-/-}$ mice, CR was also expressed, but the number of CR$^+$ neurons was reduced to 51.4%, 63.1%, 54.3% and 77.7% at E14.5, E15.5, E18.5 and P0, respectively, as compared with that in wild type (see Fig. S1D-G in the supplementary material).

In summary, these results suggest that Runx3 is required for both the appearance of PV expression and the maintenance of TrkC expression until E13.5, but not for the initial appearance of TrkC.

Projection of proprioceptive DRG afferents in *Runx3*$^{-/-}$ mice

Because the expression of PV and TrkC was lost or decreased in *Runx3*$^{-/-}$ mice, we next analyzed the axonal projection of these neurons. We also analyzed Vglut1 (Slc17a7) expression, as a marker for a subpopulation of proprioceptive DRG neurons (Alvarez et al., 2004; Landry et al., 2004).

TrkC$^+$ afferents projected to the dorsal horn, the intermediate zone and the ventral horn of the spinal cord in P0 wild-type mice. In *Runx3*$^{-/-}$ mice, however, the projection to the dorsal horn was observed, but not to the intermediate zone and the ventral horn (Fig. 4A). PV$^+$ afferents projected to the ventral horn through the dorsal horn in the wild-type mice at P0. In *Runx3*$^{-/-}$ mice, no projection to the spinal cord was observed throughout developmental stages from E14.5 to P0 (Fig. 4B, data not shown). Vglut1$^+$ afferents projected to the deep layer of the dorsal horn, the intermediate zone and the ventral horn in the wild-type mice, whereas the projection to the ventral horn was not observed in *Runx3*$^{-/-}$ mice (Fig. 4C).

To investigate whether the loss of projections to the ventral horn in *Runx3*$^{-/-}$ mice results from the apoptosis of proprioceptive DRG neurons, we examined the projections of DRG afferents using DiI labeling in *Runx3*$^{-/-}$; *Bax*$^{-/-}$ mice and *Runx3*$^{+/+}$; *Bax*$^{-/-}$ mice at P0. DiI-labeled afferents projected to the ventral horn of the spinal cord in *Runx3*$^{+/+}$; *Bax*$^{-/-}$ mice, but not in *Runx3*$^{-/-}$; *Bax*$^{-/-}$ mice (see Fig. S2 in the supplementary material), suggesting that the disappearance of proprioceptive DRG afferents is not due to apoptosis of the DRG neurons.

Next, we identified the TrkC$^+$ neurons by examining the co expression of cutaneous markers in the wild-type and *Runx3*$^{-/-}$ mice at P0. In the skin of the lower limb, the co expression of TrkC and TrkA (Fig. 4D,E), and of TrkC and CGRP (Fig. 4F,G), were observed in some fibbers of both the wild-type and *Runx3*$^{-/-}$ mice. In the DRG, some TrkC$^+$ neurons coexpressed CGRP or TrkB, both in the wild-type and *Runx3*$^{-/-}$ mice (see Fig. S3 in the supplementary material). In the muscle, however, TrkC$^+$ and PV$^+$ afferents were observed in wild-type but not in *Runx3*$^{-/-}$ mice (Fig. 4H-J, data not shown).

In summary, these results suggest that Runx3 is required for the proper projection of proprioceptive afferents. In addition, TrkC$^+$ neurons observed in *Runx3*$^{-/-}$ mice may subserve cutaneous sensation.

Expression of various markers of DRG neuron subtypes

As mentioned above, the number of Islet1$^+$ neurons was reduced by as much as 1300 in the *Runx3*$^{-/-}$ mice at P0, but only a limited decrease of TrkC$^+$, PV$^+$ and CR$^+$ neurons was detected. To clarify the participation of other types of neurons in this decrease, we examined the number of Vglut1$^+$ neurons as the subpopulation of proprioceptive DRG neurons, and TrkA$^+$, TrkB$^+$, c-Ret$^+$, calbindin-28K (CB)$^+$, somatostatin (SOM)$^+$ and CGRP$^+$ neurons as cutaneous DRG neurons (Fig. 5).

The number of Vglut1$^+$ neurons was decreased to 69% in *Runx3*$^{-/-}$ mice as compared with the wild-type mice (788.5±39.5 versus 546.2±18.7, n=6 for both *Runx3*$^{+/+}$ and *Runx3*$^{-/-}$, P<0.001) (Fig. 5A). Moreover, the number of TrkA$^+$ neurons was decreased to 69% in *Runx3*$^{-/-}$ mice (4767.2±59.7 versus 3268.5±148.8, n=6, P<0.001) (Fig. 5B), SOM$^+$ neurons to 57% (471.8±39.4 versus 268.0±13.9, n=6, P<0.01) (Fig. 5F) and CGRP$^+$ neurons to 82% (804.2±31.6 versus 659.0±29.7, n=6, P<0.01) (Fig. 5G). TrkB$^+$ neurons were decreased, but not significantly (1484.2±133.0 versus 1207.7±134.3, n=6, P=0.067) (Fig. 5C). By contrast, the number of CB$^+$ neurons increased to 128% (510.8±17.5 versus 651.3±22.0, n=6, P<0.01) (Fig. 5E), whereas the number of c-Ret$^+$ neurons was unchanged in *Runx3*$^{-/-}$ mice (1186.0±129.0 versus 1246.5±53.4, n=6, P=0.35) (Fig. 5D). These results indicate that *Runx3* deficiency affected the expression of cutaneous marker molecules differentially in DRG neurons at P0.

Co expression of Runx3 with DRG neuron subtype markers and Runx1

To clarify whether the changes in the expression of TrkC, PV, CR, TrkA and TrkB in *Runx3*$^{-/-}$ mice were regulated cell-autonomously by Runx3, the co expression of Runx3 with these marker molecules was examined in wild-type mice.

The majority of TrkC$^+$ DRG neurons (83.0±1.3%, n=69) were Runx3-positive at E13.5 (Fig. 6A,C), but only one-third of TrkC$^+$ neurons coexpressed Runx3 at P0 (30.1±3.0%, n=17, P<0.001)

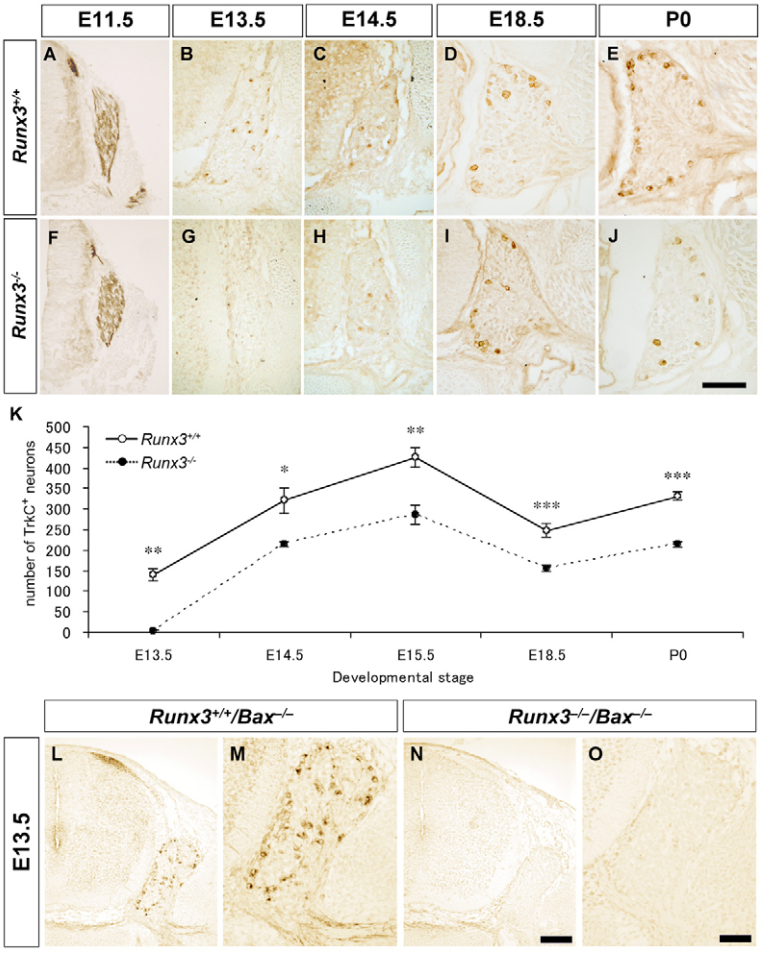

Fig. 3. Transient loss of TrkC expression in *Runx3*$^{-/-}$ DRGs during development. (**A-J**) Photomicrographs showing TrkC immunoreactivity (brown) at E11.5 (A,F), E13.5 (B,G), E14.5 (C,H), E18.5 (D,I) and P0 (E,J) in wild-type (A-E) and *Runx3*$^{-/-}$ (F-J) DRGs at the level of Th10. (**K**) Quantification of TrkC^{+} DRG neurons from E13.5 to P0. The number of TrkC^{+} DRG neurons was consistently smaller in *Runx3*$^{-/-}$ (black circles) than in wild type (white circles) mice between E13.5 and P0. (**L-O**) Immunoreactivity of TrkC in *Runx3*$^{+/+}$; *Bax*$^{-/-}$ (L,M) and in *Runx3*$^{-/-}$; *Bax*$^{-/-}$ (N,O) DRGs at the level of Th10. The DRGs of L and N are shown at higher magnification in M and O, respectively. TrkC was expressed in *Runx3*$^{+/+}$; *Bax*$^{-/-}$ DRG neurons but not in *Runx3*$^{-/-}$; *Bax*$^{-/-}$ DRG neurons. Data are shown as mean ±s.e.m.; **P*<0.05, ***P*<0.01, ****P*<0.001. Scale bars: 100 μm in J and in N for L,N; 50 μm in O for M,O.

(Fig. 6B,C). By contrast, almost all PV^{+} neurons coexpressed Runx3 and TrkC (Fig. 6D), whereas CR^{+} neurons coexpressed TrkC but not Runx3 at P0 (see Fig. S4 in the supplementary material). Moreover, the subpopulation of TrkA^{+} and TrkB^{+} neurons coexpressed Runx3 at P0 (Fig. 6E,F). These findings suggest that Runx3 might regulate the expression of TrkC, PV, TrkA and TrkB cell-autonomously.

We also investigated the co expression of Runx3 and Runx1 in wild-type mice. Few Runx3^{+} DRG neurons coexpressed Runx1 at E16.5, but almost all Runx3^{+} neurons coexpressed Runx1 at E18.5 and P0 (Fig. 6G,H; data not shown). These findings revealed that Runx3 expression changes dynamically during development, suggesting that Runx3 might function in concert with Runx1 in DRG neuron subsets at late developmental stages.

DISCUSSION

In the present study, to clarify the roles of Runx3 in the development of DRG neurons, we analyzed neuronal profiles and axonal projections in *Runx3*$^{-/-}$ mice using immunohistochemistry for specific neuronal subtype markers. We found that TrkC^{+} DRG neurons consist of two subpopulations: an early-developing subpopulation that maintains TrkC expression until E13.5 depending on Runx3; and a late-developing subpopulation that starts TrkC expression from E14.5 independently of Runx3. From the analysis of the axonal projections to central and peripheral targets, it could be suggested that early-developing Runx3-dependent TrkC^{+} DRG neurons may subserve proprioception, whereas late-developing Runx3-independent neurons may subserve cutaneous sensation. We also provide evidence that Runx3 positively regulates the expression of TrkA, CGRP and SOM, as well as TrkC, PV, CR and Vglut1, suggesting that Runx3 might be involved in the development of cutaneous, as well as proprioceptive, DRG neurons. Considering our previous study reporting the negative regulation of TrkA, CGRP, SOM and TrkC by Runx1 (Yoshikawa et al., 2007), it can be suggested that Runx1 and Runx3 have antagonistic roles in the development of DRG neuron subsets.

Proprioceptive DRG neurons are lost from the onset of development under *Runx3* deficiency

Several lines of evidence have suggested that Runx3 plays a crucial role in the cell fate specification of proprioceptive DRG neurons (Inoue et al., 2002; Levanon et al., 2002; Kramer et al., 2006). The expression of PV, a specific marker for proprioceptive DRG neurons (Copray et al., 1994; Honda, 1995), was not detected in DRGs of *Runx3*$^{-/-}$ newborn mice (Inoue et al., 2002; Levanon et al., 2002). The present study confirmed the loss of PV^{+} DRG neurons in *Runx3*$^{-/-}$ mice at P0 and further showed that PV^{+} DRG neurons were virtually absent from *Runx3*$^{-/-}$ mice from E13.5 to P0, whereas PV^{+} DRG neurons appeared by E13.5 in the wild-type mice (Fig. 2). Therefore, the present study suggests that Runx3 is required for the induction of PV expression, and it is likely that proprioceptive DRG neurons fail to develop from the onset under *Runx3* deficiency.

The loss of proprioceptive DRG neurons in *Runx3*$^{-/-}$ mice was also supported by the absence of axonal projections to the central and peripheral targets (Inoue et al., 2002; Levanon et al., 2002) (the

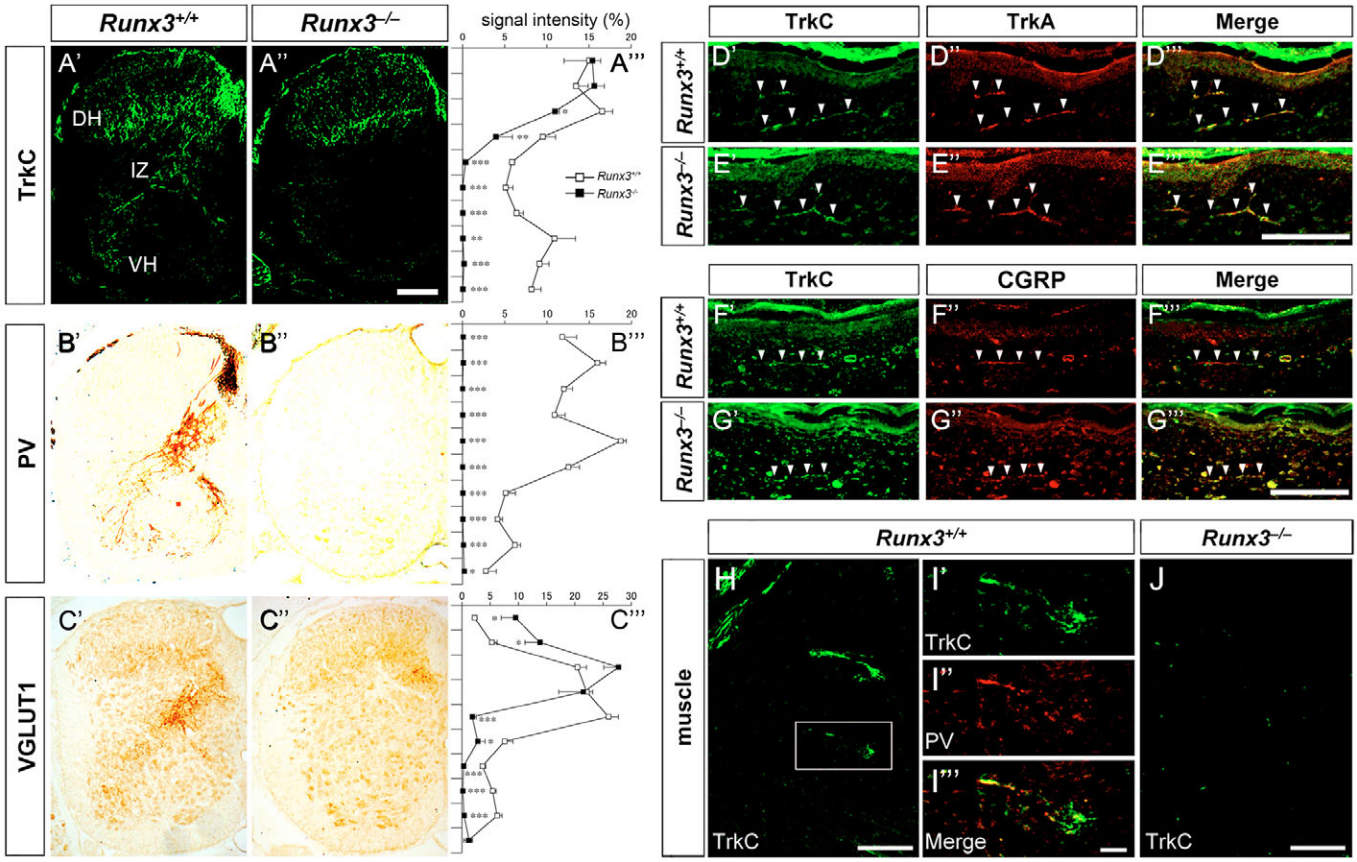

Fig. 4. DRG axon projections to the spinal cord, skin and muscle in wild-type and *Runx3*$^{-/-}$ mice at P0. (**A-C**) Representative photomicrographs of the immunoreactivity of TrkC (A′,A″; green), PV (B′,B″; brown) and Vglut1 (C′,C″; brown) in the spinal cord of wild-type (A′-C′) and *Runx3*$^{-/-}$ (A″-C″) mice. The spinal cords shown in A and B were from the same littermates, those in C from different littermates. The relative signal intensity of the immunoreactivity of TrkC (A‴), PV (B‴) and Vglut1 (C‴) in the spinal cords along the dorsoventral axis in wild-type (white squares) and *Runx3*$^{-/-}$ (black squares) mice. In total, six spinal cord sections from two to three animals of each genotype were analyzed. TrkC^{+} afferents project to the dorsal horn (DH), the intermediate zone (IZ) and the ventral horn (VH) in the wild-type mice (A′,A‴), but not to the intermediate zone and the ventral horn in *Runx3*$^{-/-}$ mice (A″,A‴). PV^{+} afferents project to the ventral horn in the wild-type (B′,B‴), but not in *Runx3*$^{-/-}$ mice (B″,B‴). Vglut1^{+} afferents project to the dorsal horn, the intermediate zone and the ventral horn in the wild type (C′,C‴), but not to the ventral horn in *Runx3*$^{-/-}$ mice (C″,C‴). (**D-G**) Double staining of TrkC^{+} (D′,E′; green) and TrkA^{+} (D″,E″; red), and of TrkC^{+} (F′,G′; green) and CGRP^{+} (F″,G″; red) axons in the skin of wild-type (D,F) and *Runx3*$^{-/-}$ (E,G) mice from the same littermates. Arrowheads indicate TrkC^{+}/TrkA^{+} or TrkC^{+}/CGRP^{+} axons (yellow in D‴-G‴). (**H-J**) Immunoreactivity of TrkC (H,I″; green) and PV (I″; red) in the muscle of wild-type mice (merge in I‴), and of TrkC (J; green) in *Runx3*$^{-/-}$ mice. TrkC^{+} axons project to the muscle in wild-type but not in *Runx3*$^{-/-}$ mice. PV immunoreactivity was not observed in the muscle of *Runx3*$^{-/-}$ mice (data not shown). Data are shown as mean ±s.e.m.; **P*<0.05, ***P*<0.01, ****P*<0.001. Scale bars: 100 μm in A″,H,J; 50 μm in E‴,G‴; 20 μm in I‴.

present study). In the present study, PV^{+}, TrkC^{+} and Vglut1^{+} afferents did not extend to the ventral horn in *Runx3*$^{-/-}$ mice, whereas these afferents projected to the ventral horn in the wild-type mice (Fig. 4A-C). In accordance with the central projection, no TrkC^{+} afferents projected to the muscle in *Runx3*$^{-/-}$ mice (Fig. 4H-J). The loss of proprioceptive DRG neurons and their axonal projections in *Runx3*$^{-/-}$ mice may not be caused by apoptosis, as no proprioceptive neuron-specific markers and axonal projections were observed in *Runx3*$^{-/-}$*; Bax*$^{-/-}$ double-knockout mice, in which DRG neurons were rescued from apoptosis during embryonic development (White et al., 1998). A recent study has shown that Runx3 regulates the axon guidance of proprioceptive DRG neurons (Chen et al., 2006a). Gain- and loss-of-function studies in chick embryos revealed that Runx3 activity determines the axonal projections to the ventral horn, the intermediate zone and the dorsal horn in the spinal cord.

Dynamic regulation of TrkC expression by Runx3

There seems to be some inconsistency regarding TrkC expression in *Runx3*$^{-/-}$ DRG neurons. Levanon et al. showed that *Runx3*$^{-/-}$ DRG neurons begin to express TrkC initially, and then lose the TrkC expression completely by E13.5 (Levanon et al., 2002). By contrast, Inoue et al. demonstrated that *Runx3*$^{-/-}$ DRG neurons maintained both TrkC immunoreactivity at E14.0 and *TrkC* mRNA expression at P0 (Inoue et al., 2002). The present study examined in detail TrkC expression in DRGs from E11.5 to P0. TrkC was expressed in DRGs of both wild-type and *Runx3*$^{-/-}$ mice at E11.5, as shown in the previous study (Levanon et al., 2002). In contrast to the continuous TrkC expression in the wild-type DRG, we found that TrkC^{+} DRG neurons disappeared completely by E13.5 in *Runx3*$^{-/-}$ mice, and then TrkC expression resumed by E14.5 to be maintained through P0. Therefore, the present study revealed that Levanon et al. and Inoue et al. observed different aspects of the dynamic TrkC

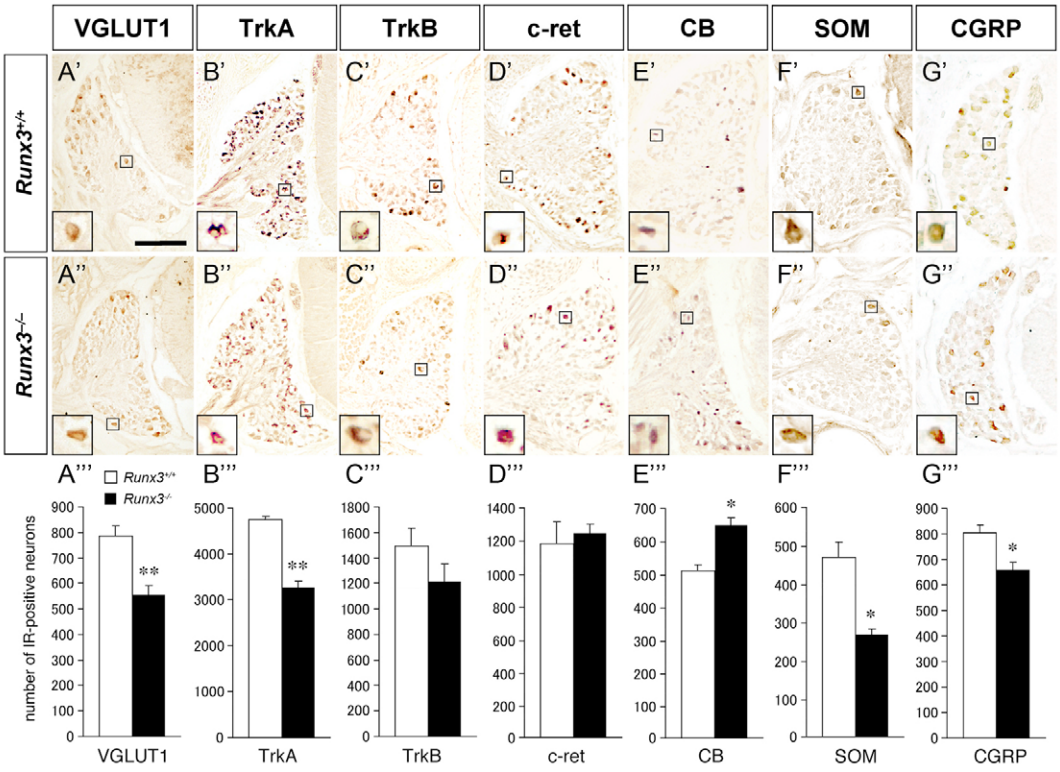

Fig. 5. Changes in the number of DRG neuron subtypes in *Runx3*$^{-/-}$ mice. (**A-G**) Immunoreactivity (brown) of Vglut1 (A′,A″), TrkA (B′,B″), TrkB (C′,C″), c-Ret (D′,D″), calbindin-28K (CB; E′,E″), somatostatin (SOM; F′,F″) and CGRP (G′,G″) in wild-type (A′-G′) and *Runx3*$^{-/-}$ (A″-G″) mice. Boxed areas of immunoreactive neurons are shown at higher magnification in the insets at the left bottom of each panel. (A‴-G‴) Quantification of the number of DRG neuron subtypes in wild-type (white bars) and *Runx3*$^{-/-}$ (black bars) mice. Data are shown as mean ±s.e.m.; **P*<0.05, ***P*<0.001. Scale bar: 100 μm.

expression in *Runx3*$^{-/-}$ DRGs: the initial appearance of TrkC expression, its transient loss and recovery. We also showed that the disappearance of TrkC^{+} DRG neurons in E13.5 *Runx3*$^{-/-}$ mice is not due to apoptosis, as TrkC expression was maintained in *Runx3*$^{+/+}$; *Bax*$^{-/-}$ but not in *Runx3*$^{-/-}$; *Bax*$^{-/-}$ DRGs at E13.5 (Fig. 3L-O). Therefore, the present study showed that Runx3 is required for the maintenance of TrkC expression until E13.5.

Although TrkC expression recovered by E14.5, our quantitative analysis revealed a constant decrease in the number of TrkC^{+} DRG neurons in *Runx3*$^{-/-}$ from E13.5 to P0, as compared with wild type (Fig. 3). The reduction in the number of TrkC^{+} neurons (by 100-150) in *Runx3*$^{-/-}$ mice was comparable to the number of PV^{+} DRG neurons in the wild-type mice (Fig. 2G, Fig. 3K). Considering that almost all PV^{+} DRG neurons coexpressed TrkC (Fig. 6De), the TrkC^{+} DRG neurons lost in *Runx3*$^{-/-}$ mice may correspond to TrkC^{+}/PV^{+} proprioceptive neurons. We also investigated the coexpression of Runx3 and TrkC in wild-type mice, and showed that most TrkC^{+} DRG neurons coexpressed Runx3 at E13.5, whereas about 30% of TrkC^{+} neurons coexpressed Runx3 at P0 (Fig. 6A-C). This level of coexpression in the wild-type mice at P0 was almost comparable to the reduction (by ~35%) in the number of TrkC^{+} DRG neurons in *Runx3*$^{-/-}$ mice at P0. Taken together, it is likely that Runx3 is required for the maintenance of the initial TrkC expression and the proper development of proprioceptive neurons.

In *Runx3*$^{-/-}$ mice, a subset of DRG neurons recovers TrkC expression independently of Runx3 from E14.5 (Fig. 3). Because these later-appearing TrkC^{+} DRG neurons projected to the dorsal spinal cord and the skin and coexpressed markers of cutaneous DRG neurons, such as TrkA and CGRP, these neurons seem to be cutaneous in nature. Indeed, previous studies have shown that a subset of TrkC^{+} DRG neurons send axons to the skin (Bronzetti et al., 1995; McMahon et al., 1994; Oakley and Karpinski, 2002; Oakley et al., 2000). The expression of TrkC in non-proprioceptive DRG neurons has also been reported (Genç et al., 2004). Erzurumlu's group examined neurotrophin 3 (*Ntf3*) knockout mice and found that no DRG neurons express TrkC at E15, but TrkC^{+} DRG neurons appear at P0, although these do not express PV (Genç et al., 2004). Considering that *Ntf3* knockout mice lack proprioceptive DRG neurons (Ernfors et al., 1994; Fariñas et al., 1994), these TrkC^{+}/PV^{-} DRG neurons should be other than proprioceptive neurons. Taken together, it seems likely that TrkC expression around E13.5 is regulated by Runx3, and that during the critical period TrkC plays pivotal roles in the proper cell fate specification of proprioceptive neurons.

Runx3 regulates the expression of cutaneous DRG neuron-specific markers

We demonstrated that the total number of DRG neurons was greatly reduced (by as much as 1300) in *Runx3*$^{-/-}$ mice at P0 (Fig. 1C). The reduction of DRG neurons at P0 was not affected by caspase 3-dependent apoptosis (Fig. 1E-G). Because the magnitude of this reduction cannot be explained by the loss of PV^{+} (nearly 150), TrkC^{+} (nearly 150) and/or Vglut1^{+} (nearly 250) proprioceptive DRG neurons, we examined the number of TrkA^{+}, TrkB^{+}, CB^{+}, CGRP^{+}, SOM^{+}, c-Ret^{+} cutaneous DRG neurons. We found that DRG neurons that express TrkA, CGRP and SOM were decreased by nearly 1500, 150 and 200 in *Runx3*$^{-/-}$ mice, respectively (Fig. 5). TrkB^{+} DRG

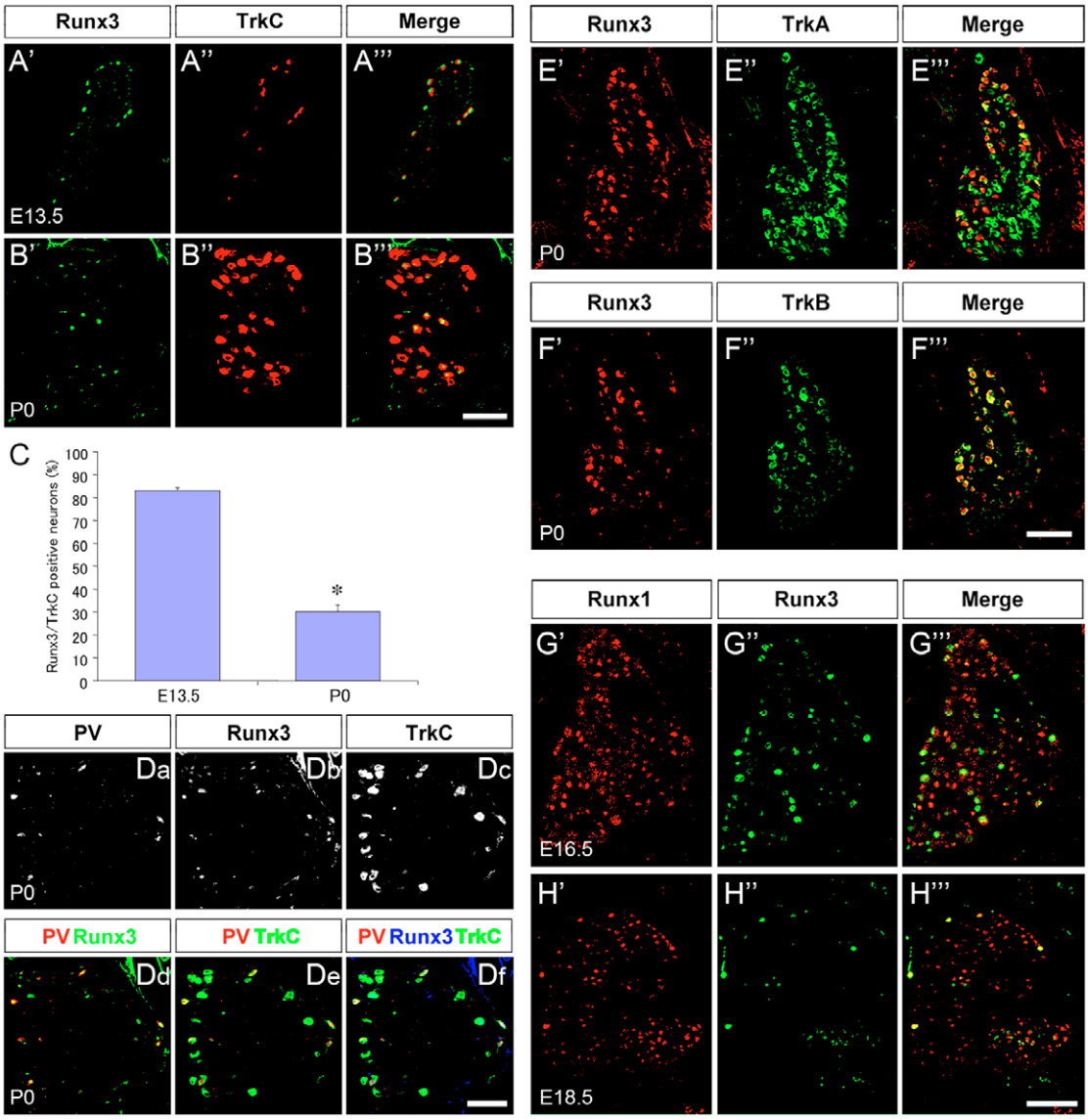

Fig. 6. Coexpression of Runx3 and neuron subtype markers in the wild-type DRG. (**A**,**B**) Double staining of Runx3 (A′,B′; green) and TrkC (A″,B″; red) at E13.5 (A) and P0 (B) in Th9 DRGs; (A‴,B‴) merge. (**C**) The ratio of Runx3$^+$/TrkC$^+$ DRG neurons at E13.5 and P0. (**D**) Triple staining of PV (a), Runx3 (b) and TrkC (c) in Th9 DRGs at P0; (d-f) merges. Some images are shown with pseudo coloring (A,B,D). (**E**,**F**) Double staining of Runx3 (red) in combination with TrkA (green) (E) and TrkB (green) (F) in Th10 DRGs at P0. (**G**,**H**) Double staining of Runx3 (green) and Runx1 (red) at E16.5 (G) and E18.5 (H) in Th10 DRGs. Data are shown as mean ± s.e.m.; *P<0.001. Scale bars: 100 μm.

neurons seemed to be decreased, but no significant difference was detected. By contrast, the number of CB$^+$ DRG neurons was increased, whereas that of c-Ret$^+$ neurons was unchanged in *Runx3*$^{-/-}$ mice. The expression of c-Ret may be regulated by Runx1, because the number of c-Ret$^+$ DRG neurons was increased in *Runx1*$^{-/-}$ mice (Chen et al., 2006b; Yoshikawa et al., 2007).

The present studies suggest that Runx3 might be involved in the development of subsets of cutaneous DRG neurons as well as proprioceptive neurons, by regulating the expression of TrkA, CB, SOM and CGRP. Unfortunately, functions of cutaneous sensation cannot be analyzed in *Runx3*$^{-/-}$ mice because they die shortly after birth. In addition, the regulatory mechanisms underlying the expression of these molecules by Runx3 are not well known. There seem to be two possibilities: cell-autonomous regulation and indirect regulation. In vivo analysis of the coexpression of Runx3 with these molecules during development and loss- and gain-of-function studies are needed to reveal the regulatory mechanisms of Runx3. It is possible that the regulation of TrkA and TrkB by Runx3 is cell-autonomous, because a subpopulation of TrkA$^+$ and TrkB$^+$ DRG neurons coexpressed Runx3 (Fig. 6E,F). It has been reported that *Runx3* transcriptionally represses TrkB expression and that TrkB$^+$ DRG neurons increased from E11 to E13 but not at later embryonic stages in *Runx3*$^{-/-}$ mice (Kramer et al., 2006; Inoue et al., 2007). In contrast to this increase of TrkB$^+$ DRG neurons in *Runx3*$^{-/-}$ mice during early embryonic stages, the present study showed that these neurons tended to decrease in *Runx3*$^{-/-}$ mice at birth. The tendency at P0 might result from cell death due to the mismatch of neurotrophic factors between overproduced TrkB$^+$ DRG neurons and their axonal targets (Oppenheim, 1991).

Runx3 and Runx1 have antagonistic effects on the development of subsets of DRG neurons

The present study showed that the total number of DRG neurons was decreased in P0 *Runx3*$^{-/-}$ mice. It is interesting to see that the total number of DRG neurons increases in *Runx1*$^{-/-}$ mice (Chen et al., 2006b; Yoshikawa et al., 2007). Furthermore, the present study showed that the number of TrkA^{+}, CGRP^{+}, SOM^{+} and TrkC^{+} neurons was decreased in *Runx3*$^{-/-}$ mice, suggesting that Runx3 positively regulates the expression of TrkA, CGRP, SOM and TrkC. In striking contrast, we have previously shown that DRG neurons that express TrkA, CGRP, SOM and TrkC were increased in *Runx1*$^{-/-}$ mice (Yoshikawa et al., 2007). These results suggest that Runx1 and Runx3 might be involved antagonistically in the development of subsets of DRG neurons. Further studies that include their downstream targets will be needed to understand the roles of Runx1 and Runx3.

We thank Drs M. Watanabe and F. Reichardt for providing antibodies against Vglut1 and TrkA, respectively. This study was supported by Grant-in-Aid for Scientific Research from the 21st Century COE Program from the Ministry of Education, Culture, Sports, Science and Technology (MEXT) of Japan to M.Y., S.O. and T.S., and Grant-in-Aid for Young Scientists (B) to K.S. from MEXT.

Supplementary material

Supplementary material for this article is available at
http://dev.biologists.org/cgi/content/full/135/9/1703/DC1

References

Alvarez, F. J., Villalba, R. M., Zerda, R. and Schneider, S. P. (2004). Vesicular glutamate transporters in the spinal cord, with special reference to sensory primary afferent synapses. *J. Comp. Neurol.* **472**, 257-280.

Bibel, M. and Barde, Y. A. (2000). Neurotrophins: key regulators of cell fate and cell shape in the vertebrate nervous system. *Genes Dev.* **14**, 2919-2937.

Bronzetti, E., Ciriaco, E., Germana, G. and Vega, J. A. (1995). Immunohistochemical localization of neurotrophin receptor proteins in human skin. *Ital. J. Anat. Embryol.* **100**, 565-571.

Chen, A. I., de Nooij, J. C. and Jessell, T. M. (2006a). Graded activity of transcription factor Runx3 specifies the laminar termination pattern of sensory axons in the developing spinal cord. *Neuron* **49**, 395-408.

Chen, C. L., Broom, D. C., Liu, Y., de Nooij, J. C., Li, Z., Cen, C., Samad, O. A., Jessell, T. M., Woolf, C. J. and Ma, Q. (2006b). Runx1 determines nociceptive sensory neuron phenotype and is required for thermal and neuropathic pain. *Neuron* **49**, 365-377.

Coffman, J. A. (2003). Runx transcription factors and the developmental balance between cell proliferation and differentiation. *Cell Biol. Int.* **27**, 315-324.

Copray, J. C., Mantingh-Otter, I. J. and Brouwer, N. (1994). Expression of calcium-binding proteins in the neurotrophin-3-dependent subpopulation of rat embryonic dorsal root ganglion cells in culture. *Brain Res. Dev. Brain Res.* **81**, 57-65.

Ernfors, P., Lee, K.-E., Kucera, J. and Jaenish, R. (1994). Lack of neurotrophin-3 leads to deficiencies in the peripheral nervous system and loss of limb proprioceptive afferents. *Cell* **77**, 503-512.

Fariñas, I., Jones, K. R., Backus, C., Wang, X. Y. and Reichardt, L. F. (1994). Severe sensory and sympathetic deficits in mice lacking neurotrophin-3. *Nature* **369**, 658-661.

Genç, B., Özdinler, P. H., Mendoza, A. E. and Erzurumlu, R. S. (2004). A chemoattractant role for NT-3 in proprioceptive axon guidance. *PLoS Biol.* **2**, 2112-2121.

Honda, C. N. (1995). Differential distribution of calbindin-D28k and parvalbumin in somatic and visceral sensory neurons. *Neuroscience* **68**, 883-892.

Huang, E. J. and Reichardt, L. F. (2001). Neurotrophins: roles in neuronal development and function. *Annu. Rev. Neurosci.* **24**, 677-736.

Inoue, K., Ozaki, S., Shiga, T., Ito, K., Masuda, T., Okado, N., Iseda, T., Kawaguchi, S., Ogawa, M., Bae, S. C. et al. (2002). Runx3 controls the axonal projection of proprioceptive dorsal root ganglion neurons. *Nat. Neurosci.* **5**, 946-954.

Inoue, K., Ito, K., Osato, M., Lee, B., Bae, S. C. and Ito, Y. (2007). The transcription factor Runx3 represses the neurotrophin receptor TrkB during lineage commitment of dorsal root ganglion neurons. *J. Biol. Chem.* **282**, 24175-24184.

Ito, Y. (2004). Oncogenic potential of the RUNX gene family: overview. *Oncogene* **23**, 4198-4208.

Knudson, C. M., Tung, K. S., Tourtellotte, W. G., Brown, G. A. and Korsmeyer, S. J. (1995). Bax-deficient mice with lymphoid hyperplasia and male germ cell death. *Science* **270**, 96-99.

Kramer, I., Sigrist, M., de Nooij, J. C., Taniuchi, I., Jessell, T. M. and Arber, S. (2006). A role for Runx transcription factor signaling in dorsal root ganglion sensory neuron diversification. *Neuron* **49**, 379-393.

Kucera, J., Cooney, W., Que, A., Szeder, V., Stancz-Szeder, H. and Walro, J. (2002). Formation of supernumerary muscle spindles at the expense of Golgi tendon organs in ER81-deficient mice. *Dev. Dyn.* **223**, 389-401.

Landry, M., Bouali-Benazzouz, R., El Mestikawy, S., Ravassard, P. and Nagy, F. (2004). Expression of vesicular glutamate transporters in rat lumbar spinal cord, with a note on dorsal root ganglia. *J. Comp. Neurol.* **468**, 380-394.

Levanon, D., Brenner, O., Negreanu, V., Bettoun, D., Woolf, E., Eilam, R., Lotem, J., Gat, U., Otto, F., Speck, N. et al. (2001). Spatial and temporal expression pattern of Runx3 (Aml2) and Runx1 (Aml1) indicates non-redundant functions during mice embryogenesis. *Mech. Dev.* **109**, 413-417.

Levanon, D., Bettoun, D., Harris-Cerruti, C., Woolf, E., Negreanu, V., Eilam, R., Bernstein, Y., Goldenberg, D., Xiao, C., Fliegauf, M. et al. (2002). The Runx3 transcription factor regulates development and survival of TrkC dorsal root ganglia neurons. *EMBO J.* **21**, 3454-3463.

Li, Q. L., Ito, K., Sakakura, C., Fukamachi, H., Inoue, K., Chi, X. Z., Lee, K. Y., Nomura, S., Lee, C. W., Han, S. B. et al. (2002). Causal relationship between the loss of RUNX3 expression and gastric cancer. *Cell* **109**, 113-124.

Markus, A., Patel, T. D. and Snider, W. D. (2002). Neurotrophic factors and axonal growth, *Curr. Opin. Neurobiol.* **12**, 523-531.

Marmigère, F. and Ernfors, P. (2007). Specification and connectivity of neuronal subtypes in the sensory lineage. *Nat. Rev. Neurosci.* **8**, 114-127.

Marmigère, F., Montelius, A., Wegner, M., Groner, Y., Reichardt, L. F. and Ernfors, P. (2006). The Runx1/AML1 transcription factor selectively regulates development and survival of TrkA nociceptive sensory neurons. *Nat. Neurosci.* **9**, 180-187.

McMahon, S. B., Armanini, M. P., Ling, L. H. and Phillips, H. S. (1994). Expression and co expression of Trk receptors in subpopulations of adult primary sensory neurons projecting to identified peripheral targets. *Neuron* **12**, 1161-1171.

Moqrich, A., Earley, T. J., Watson, J., Andahazy, M., Backus, C., Martin-Zanca, D., Wright, D. E., Reichardt, L. F. and Patapoutian, A. (2004). Expressing TrkC from the TrkA locus causes a subset of dorsal root ganglia neurons to switch fate. *Nat. Neurosci.* **7**, 812-818.

Mu, X., Silos-Santiago, I., Carroll, S. L. and Snider, W. D. (1993). Neurotrophin receptor genes are expressed in distinct patterns in developing dorsal root ganglia. *J. Neurosci.* **13**, 4029-4041.

Oakley, R. A. and Karpinski, B. A. (2002). Target-independent specification of proprioceptive sensory neurons. *Dev. Biol.* **249**, 255-269.

Oakley, R. A., Lefcort, F. B., Plouffe, P., Ritter, A. and Frank, E. (2000). Neurotrophin-3 promotes the survival of a limited subpopulation of cutaneous sensory neurons. *Dev. Biol.* **224**, 415-427.

Oppenheim, R. W. (1991). Cell death during development of the nervous system. *Annu. Rev. Neurosci.* **14**, 453-501.

Patel, T. D., Kramer, I., Kucera, J., Niederkofler, V., Jessell, T. M., Arber, S. and Snider, W. D. (2003). Peripheral NT3 signaling is required for ETS protein expression and central patterning of proprioceptive sensory afferents. *Neuron* **38**, 403-416.

Simeone, A., Daga, A. and Calabi, F. (1995). Expression of runt in the mice embryo. *Dev. Dyn.* **203**, 61-70.

Snider, W. D. (1994). Functions of the neurotrophins during nervous system development: what the knockouts are teaching us. *Cell* **77**, 627-638.

Theriault, F. M., Roy, P. and Stifani, S. (2004). AML1/Runx1 is important for the development of hindbrain cholinergic branchiovisceral motor neurons and selected cranial sensory neurons. *Proc. Natl. Acad. Sci. USA* **101**, 10343-10348.

Theriault, F. M., Nuthall, H. N., Dong, Z., Lo, R., Barnabe-Heider, F., Miller, F. D. and Stifani, S. (2005). Role for Runx1 in the proliferation and neuronal differentiation of selected progenitor cells in the mammalian nervous system. *J. Neurosci.* **25**, 2050-2061.

White, F. A., Keller-Peck, C. R., Knudson, C. M., Korsmeyer, S. J. and Snider, W. D. (1998). Widespread elimination of naturally occurring neuronal death in Bax deficient mice. *J. Neurosci.* **18**, 1428-1439.

Yoshikawa, M., Senzaki, K., Yokomizo, T., Takahashi, S., Ozaki, S. and Shiga, T. (2007). Runx1 selectively regulates cell fate specification and axonal projections of dorsal root ganglion neurons. *Dev. Biol.* **303**, 663-674.